BER Performance of a BPSK Biomedical Telemetry System under Varying Coupling and Loading Conditions

Asimina Kiourti[1] and Andreas Demosthenous[2]

[1] National Technical University of Athens, School of Electrical & Computer Engineering
[2] University College London, Department of Electronic & Electrical Engineering
akiourti@biosim.ntua.gr, a.demosthenous@ee.ucl.ac.uk

Abstract. Binary Phase Shift Keying (BPSK) is a promising modulation format for downlink data transmission in inductive biomedical telemetry systems, because it achieves high data rates and power efficiencies and requires simple electronics. In this paper, the Bit Error Rate (BER) performance of a BPSK biomedical telemetry system is investigated under Additive White Gaussian Noise (AWGN) and is found to highly depend on the system's coupling and loading conditions. High-level simulations are presented which are indicative of the performance of a real BPSK biomedical telemetry system.

Keywords: Binary phase shift keying (BPSK), biomedical telemetry, bit error rate (BER) performance, inductive link, wireless implants.

1 Introduction

During the last decade, biomedical implanted devices have drawn great attention for both diagnosis and treatment of diseases [1], [2]. Bidirectional communication between the implant and an external control unit for data exchange and power delivery is, most commonly, performed via a wireless, transcutaneous inductive link [3]. This battery-less technique minimizes the size of the implant and eliminates patient discomfort.

The inductive link channel consists of two closely-spaced, mutually-coupled coils, one implanted and one placed outside the human body. The external unit telemeters power and modulated data (commands and stimulation parameters) to the implant (downlink transmission). Depending on the modulation format, several values of data transmission rates, error rates, delivered power and circuit complexity can be achieved. The implant can itself send data (monitoring signals) back to the external unit (uplink transmission), usually by means of load reflectance techniques [4].

Amplitude keying formats (Amplitude Shift Keying, ASK, and On-Off Keying, OOK) were the first to be used for downlink data transmission [5], [6]. However, despite their simple implementation, they were limited to deliver low amounts of power and achieve low data transmission rates. Phase Shift Keying (PSK) techniques have been proved to be the best alternative [7], [8], [9]. Binary Phase Shift Keying (BPSK) is the simplest form of PSK. A single carrier signal is modulated by controlling its polarity according to the binary data signal to be transmitted. The amplitude of

J. Lin and K.S. Nikita (Eds.): MobiHealth 2010, LNICST 55, pp. 144–150, 2011.

the BPSK modulated signal is kept constant, thus increasing the maximum power delivered to the implant. Bit rates as high as 1.12 Mbps for a carrier frequency of 13.56 MHz have been reported in literature [7].

The rest of the paper is organized as follows. In section 2, a BPSK biomedical telemetry system is designed and simulated in Simulink, Matlab [10]. Additive White Gaussian Noise (AWGN) is assumed to distort the signal while propagating in the wireless inductive link channel. In Section 3, the system's Bit Error Rate (BER) performance is evaluated under various noise levels and its dependence on the system's coupling and loading conditions is examined. The paper concludes in Section 4.

2 BPSK Telemetry System Overview

A block diagram of the BPSK biomedical telemetry circuit designed in Simulink, Matlab is illustrated in Fig. 1(a). At the external unit, the binary data are BPSK modulated and driven to a power amplifier to produce an adequate transmitting power. An ideal (theoretic power efficiency of 100%), unity-gain Class-E power amplifier is assumed [11]. Downlink data transmission takes place across the inductive link channel and BPSK demodulation is performed at the implant's side. For simplicity reasons, the implanted electronic system is modeled as an equivalent ac load resistor R_l. Three values are examined, $R_l = 300$, 1000 and 2000 Ohm. In a real system, R_l will be complex and time-varying.

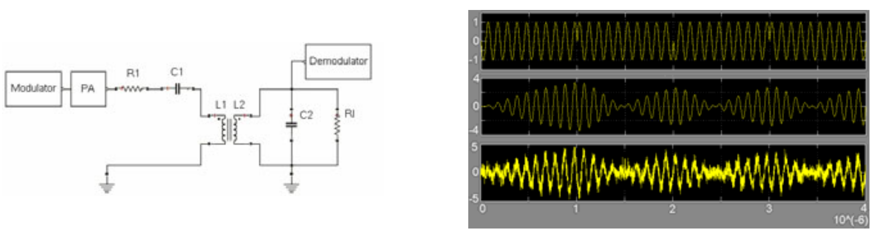

(a) (b)

Fig. 1. (a) Model of the designed BPSK biomedical telemetry system, (b) Simulated waveforms of the signals at the output of the modulator and input of the demodulator for zero and finite AWGN distortion, respectively

2.1 Inductive Link Channel

To achieve high gain while requiring low input voltages, the inductive link channel consists of a series-external (primary) and a parallel-implanted (secondary) resonant circuits [12], both tuned at the carrier frequency of $f_c = 10$ MHz, according to:

$$2\pi f_c = \frac{1}{\sqrt{L_1 C_1}} = \frac{1}{\sqrt{L_2 C_2}} , \tag{1}$$

where L_1, C_1, L_2, C_2 represent the inductor and capacitor values of the primary and secondary circuits. The carrier frequency has been chosen as a compromise between data transfer rate, power efficiency and human safety [13]. The coupling between the coils, or equivalently the proportion of the primary's flux which is linked with the secondary, is described in terms of the coupling factor, k [14]. The coupling factor depends on the geometry and distance between the coils, as well as on the material properties of the coupling medium. The resistor R_1 accounts for the ohmic losses of the external side, while the implanted side's ohmic losses are included in R_l.

The transfer function of the inductive link channel (in the Laplace domain) can be derived from the network equations of the primary and secondary resonant circuits, as:

$$\frac{V_{out}(s)}{V_i(s)} = \frac{sk^2 L_1 L_2 R_l}{\left(sL_2 + s^2 R_l L_2 C_2 + R_l\right)\left(R_1 + \frac{1}{sC_1} + sL_1\right) - s^2 k^2 L_1 L_2 \left(1 + sR_l C_2\right)}, \quad (2)$$

where V_i and V_{out} denote the signals at the input and output of the channel, respectively [7]. The inductive link channel acts as a bandpass filter centered at the resonant frequency [12] and is assumed to add Additive White Gaussian Noise (AWGN), which accounts for coil misalignments, element variations and environmental noise.

The resonant coils are considered to have equal inductances, $L_1 = L_2 = 1.25$ μH. Three typical values of the coupling factor are examined, $k = 0.03$, 0.06 and 0.1, while $R_1 = 3$ Ohm.

Example waveforms of the BPSK modulated signal at the output of the modulator and at the input of the BPSK demodulator, when the channel causes zero and finite AWGN distortion, are shown in Fig. 1(b), respectively, for the case where $k = 0.06$ and $R_l = 300$ Ohm.

2.2 BPSK Modulator

The designed BPSK modulator circuit is illustrated in Fig. 2(a). Random binary digits are produced at a rate of 1 Mbps and are converted into a binary bipolar PAM signal, where "1" and "0" bits are represented as 1 V and −1 V voltage levels, respectively. The bipolar PAM signal is subsequently multiplied with a sinusoidal carrier signal of unity amplitude, to produce the BPSK modulated signal:

$$m(t) = \begin{cases} \sin\left(2\pi f_c t\right) & \text{"1" bit} \\ -\sin\left(2\pi f_c t\right) & \text{"0" bit} \end{cases}. \quad (3)$$

Power is delivered to the implant through the energy contained in the incoming BPSK modulated signal, via power rectification and regulation circuits found on the implant's side [15], [16]. As a result, the BPSK modulator serves the dual purpose of data transmission and power delivery. Fig. 2(b) illustrates the simulated waveforms of the first four bits to be transmitted, the carrier signal, and the corresponding BPSK modulated signal, respectively.

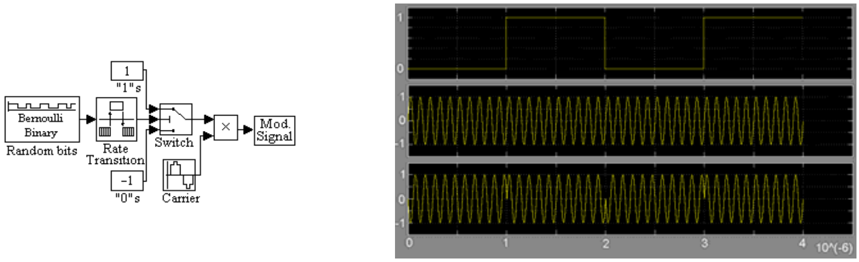

(a) (b)

Fig. 2. (a) Model of the designed BPSK modulator circuit, and (b) Simulated waveforms of the first four bits to be transmitted, the carrier signal, and the corresponding BPSK modulated signal

2.3 BPSK Demodulator

A simplified coherent BPSK demodulator circuit was designed, as depicted in Fig. 3(a). The received BPSK signal is multiplied with a recovered version of the carrier (most commonly obtained via a Costas loop circuit [17]) and is low-pass-filtered by means of Butterworth low-pass-filter (LPF), with a passband edge frequency of 1 MHz. The resulting signal is driven to a bit recovery circuit which consists of a sample-and-hold and a zero-threshold detector circuits, to recover the received bits.

Simulated waveforms of the signals at the input and output of the LPF and the respective recovered bits for a time period of 6 μsec are illustrated in Fig. 3(b), respectively.

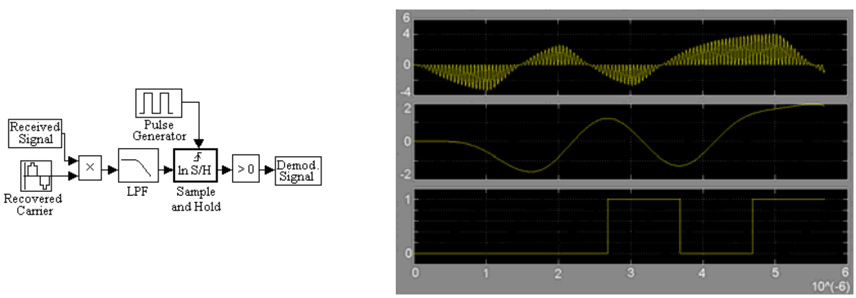

(a) (b)

Fig. 3. (a) Model of the designed BPSK demodulator circuit, and (b) Simulated waveforms of the signals at the input and output of the LPF and the respective recovered bits for a time period of 6 μsec

3 Simulation Results

Stand-alone C code was generated and executed in Real Time Workshop [18] to simulate the transmission of 1.000.000 bits through the designed BPSK telemetry system under various noise conditions. The transmitted and recovered bits were compared by means of a logical XOR gate and the number of bit errors was calculated.

The effect of coupling and loading conditions on the system's BER performance is shown in Fig. 4(a) and 4(b), respectively. The x-axis of the plots represents the signal-to-noise ratio (SNR) per bit, defined as the E_b / N_0 ratio, where E_b is the energy per bit at the input of the inductive link channel and N_0 is the noise power spectral density, related to the AWGN's variance, σ^2, as $N_0 = 2\sigma^2$. The y-axis indicates the probability of error, or equivalently the BER. The BER performance of an all-pass, unity-gain channel linking the BPSK modulator and demodulator circuits is also depicted, for reference.

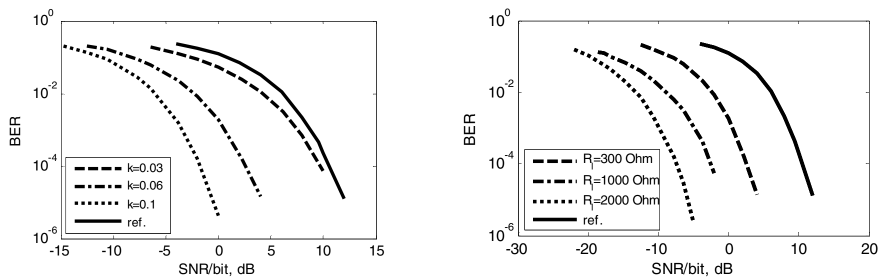

(a) (b)

Fig. 4. BER for varying (a) coupling ($R_l = 300$ Ohm) and (b) loading ($k = 0.03$) conditions

The results of Fig. 4 can be attributed to the effect of the inductive channel on the BPSK modulated signal at its input. The simulated magnitude transfer functions for the cases under study are illustrated in Fig. 5.

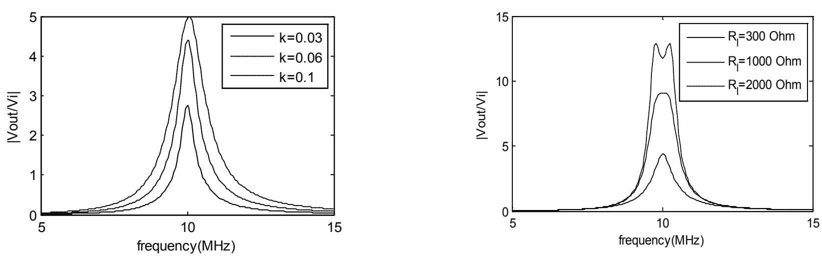

(a) (b)

Fig. 5. Inductive link magnitude transfer functions for varying (a) coupling ($R_l = 300$ Ohm) and (b) loading ($k = 0.03$) conditions

According to Fig. 5, the inductive link acts as a bandpass filter (as stated earlier), which amplifies the signals at its resonant frequency of 10 MHz. The enhancement of the inductive link's coupling factor, k , (Fig. 5(a)) and the increase of the load resistor, R_l , (Fig. 5 (b)) result in an increasingly amplified output signal. The double-peak phenomenon observed for $k = 0.06$, $R_l = 2000$ Ohm is due to the choice of the design parameters which result in the coupling factor exceeding its critical value [19].

This is indeed the case in the simulated waveforms of Fig. 6. Assuming that the modulated signal at the input of the inductive link channel is given by Eq. (3), Fig. 6(a) shows the signal at the output of the inductive link channel for $R_l = 300$ Ohm and $k = 0.03$, 0.06 and 0.1, respectively, while Fig. 6(b) shows the signal at the output of the inductive link channel for $k = 0.06$ and $R_l = 300$, 1000 and 2000 Ohm, respectively.

As a result, AWGN in the inductive link channel distorts an amplified version of the initial BPSK modulated signal, thus improving the noise performance compared to the case of an all-pass, unity-gain channel. Moreover, when k and/or R_l get higher, AWGN is added to an increasingly amplified version of the initial BPSK modulated signal, thus making the system more tolerant to AWGN distortion.

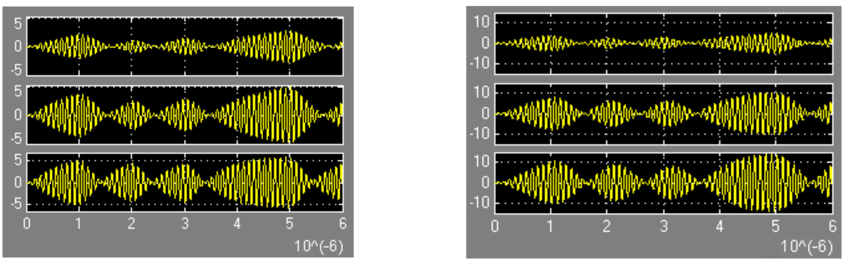

(a) (b)

Fig. 6. Simulated waveforms of the signal at the output of the inductive link channel for (a) $R_l = 300$ Ohm and $k = 0.03$, 0.06 and 0.1, respectively, and (b) $k = 0.06$ and $R_l = 300$, 1000 and 2000 Ohm, respectively

4 Conclusions

In this paper, the BER performance of a BPSK biomedical inductive telemetry system has been studied under varying coupling and loading conditions using Simulink, Matlab. High-level simulations were presented, yet provide indicative results for a real BPSK biomedical telemetry system. Better-coupled coils and heavier-loaded implants were found to increase the magnitude transfer function of the inductive link at the frequency under interest and improve the system's BER performance. Such a telemetry system can find use in cochlear implants for treatment of motion disorders, spinal canal implants for paraplegics and deep brain stimulation for the treatment of epilepsy.

Future work will include implementation and BER performance comparison with a real BPSK biomedical telemetry system. Subsequent investigations will also include investigation of the simulated BER performance of other two-level or multi-level modulation formats for downlink data transmission in biomedical telemetry systems.

Acknowledgement

The work of AK was supported by the Greek Foundation of Education and European Culture.

References

1. Sodagar, A.M., Wise, K.D., Najafi, K.: A Wireless Implantable Microsystem for Multichannel Neural Recording. IEEE Transactions on Microwave Theory and Techniques 57(10) (2009)
2. Mohseni, P., Najafi, K., Eliades, S.J., Wang, X.: Wireless Multichannel Biopotential Recording Using an Integrated FM Telemetry Circuit. IEEE Transactions on Neural Systems and Rehabilitation Engineering 13(3) (2005)
3. Sawan, M., Hu, Y., Coulombe, J.: Wireless Smart Implants Dedicated to Multichannel Monitoring and Microstimulation. IEEE Circuits & Systems Magazine 5, 21–39 (2005)
4. Tang, Z., Smith, B., Schild, J.H., Peckham, P.H.: Data transmission from an implantable biotelemeter by load-shift keying using circuit configuration modulator. IEEE Transactions on Biomedical Engineering 42(5), 524–528 (1995)
5. Liu, W., Vichienchom, K., Clements, M., DeMarco, S.C., Hughes, C., McGucken, E., Humayun, M.S., de Juan, E., Weiland, J.D., Greenberg, R.: A neuro-stimulus chip with telemetry unit for retinal prosthetic device. IEEE Journal of Solid-State Circuits 35(10), 1487–1497 (2000)
6. Gudnason, G., Bruun, E., Hauglan, M.: A chip for an implantable neural stimulator. Journal of Analog Integrated Circuits and Signal Processing 22(1), 81–89 (2000)
7. Hu, Y., Sawan, M.: A Fully Integrated Low-Power BPSK Demodulator for Implantable Medical Devices. IEEE Transactions on Circuits and Systems 52(12), 2552–2562 (2005)
8. Sonkusale, S., Luo, Z.: A Complete Data and Power Telemetry System Utilizing BPSK and LSK Signaling for Biomedical Implants. In: 30th Annual International IEEE EMBS Conference, pp. 3216–3219 (2008)
9. Deng, S., Hu, Y., Sawan, M.: A High Data Rate QPSK Demodulator for Inductively Powered Electronics Implants. In: IEEE International Symposium on Circuits and Systems, pp. 2577–2580 (2006)
10. The MathWorks, Simulink, `http://www.mathworks.com/products/simulink/`
11. Razavi, B.: RF Microelectronics. Prentice Hall, Englewood Cliffs (1998)
12. Iniewski, K.: VLSI Circuits for Biomedical Applications. Artech House, Boston (2008)
13. Valdastri, P., Menciassi, A., Arena, A., Caccamo, C., Dario, P.: An Implantable Telemetry Platform System for In Vivo Monitoring of Physiological Parameters. IEEE Transactions on Information Technology in Biomedicine 8(3) (2004)
14. Sauer, C., Stanacevic, M., Cauwenberghs, G., Thakor, N.: Power Harvesting and Telemetry in CMOS for Implanted Devices. In: IEEE International Workshop on Biomedical Circuits and Systems, pp. S1.8-1–S1.8-4 (2004)
15. Ghovanloo, M., Atluri, S.: An Integrated Full-Wave CMOS Rectifier With Built-In Back Telemetry for RFID and Implantable Biomedical Applications. IEEE Transactions on Circuits and Systems 55(10), 3328–3334 (2008)
16. Wang, G., Liu, W., Sivaprakasam, M., Kendir, G.A.: Design and Analysis of an Adaptive Transcutaneous Power Telemetry for Biomedical Implants. IEEE Transactions on Circuits and Systems 52(10) (2005)
17. Yuan, H., Hu, X., Huang, J.: Design and Implementation of Costas Loop Based on FPGA. In: 3rd IEEE Conference on Industrial Electronics and Applications, pp. 2383–2388 (2008)
18. The Mathworks, Real Time Workshop, `http://www.mathworks.com/products/rtw/`
19. Baker, M.W., Sarpeshkar, R.: Feedback Analysis and Design of RF Power Links for Low-Power Bionic Systems. IEEE Transactions on Biomedical Circuits and Systems 1(1), 28–38 (2007)